

Supporting Information: Tools for Early Prediction of Drug Loading in Lipid-Based Formulations

Linda C. Alskär,¹ Christopher J. H. Porter² and Christel A. S. Bergström^{1,2*}

1. Uppsala University Drug Optimization and Pharmaceutical Profiling Platform, Department of Pharmacy,
Uppsala University, Uppsala Biomedical Center P.O Box 580, SE-751 23 Uppsala, Sweden

2. Drug Delivery, Disposition and Dynamics, Monash Institute of Pharmaceutical Sciences, Monash University,
381 Royal Parade, Parkville, Victoria 3052, Australia

*Address correspondence to:

Christel A. S. Bergström, PhD

Uppsala University Drug Optimization and Pharmaceutical Profiling Platform

Department of Pharmacy, Uppsala University

BMC P.O. Box 580

SE-751 23 Uppsala, Sweden

Email: christel.bergstrom@farmaci.uu.se

Phone: +46 – 18 471 4118

Supporting Information

The LC-MS/MS system was a Waters Xevo TQ MS, electrospray ionization coupled to an Acquity UPLC system (Waters, Milford, MA) on a Waters BEH C18 column, 2.1 × 50 mm (1.7µm) at 60°C, with a 2 min gradient and a flow rate of 0.5 mL/min. Solvent A consisted of 5% acetonitrile and 0.1% formic acid in water, and solvent B consisted of 0.1% formic acid in acetonitrile. The LC run used a linear gradient from 0.5 to 1.2 min starting at 5% of solvent B and ending at 90%, followed by a hold from 1.2 to 1.6 min and a linear gradient to return to the initial conditions at 1.7 min. Samples were kept at 10°C until injection. The mass transitions and their respective cone voltages and collision energies are given in Table SI1.

Table SI1. Analytical conditions for compound quantification^a

compound	Retention time (min)	Parent (m/z)	CV	Daughter (m/z)	CE	Ionization
albendazole	1.25	266.1	28	234.0	20	ESI+
bezafibrate	1.39	362.1	20	139.0	26	ESI+
candesartan	1.31	441.4	18	263.2	12	ESI+
candesartan cilexetil	1.65	611.2	18	338.1	27	ESI+
dipyridamole	1.19	505.1	54	385.1	44	ESI+
glibenclamide	1.45	494.1	18	168.9	38	ESI+
haloperidol	1.28	376.1	34	165.0	24	ESI+
itraconazole	1.54	705.0	46	392.1	34	ESI+
noscapine	1.13	414.2	32	205.1	42	ESI+
praziquantel	1.39	313.1	20	203.0	16	ESI+
sulfasalazine	1.25	399.0	32	119.0	42	ESI+
toltrazuril ^b	1.52	424.1	28	-	-	ESI-

^a Cone voltage (CV), collision energy (CE), electrospray ionization (ESI) ^b No detectable daughters were present for Toltrazuril; for analyses the parent compound was used.

Table S12. Experimentally determined thermodynamic solubility in the surfactants Cremophor EL ($\leq 3\%$ w/w water) and Cremophor ELP ($\leq 0.5\%$ w/w water) at 37°C^a

compound	Cremophor EL (mg/g)	Cremophor ELP (mg/g)
acitretin	2.85 ± 0.14	1.58 ± 0.08
albendazole	2.75 ± 0.14	nd
bezafibrate	37.9 ± 5.23	14.6 ± 1.81
candesartan	11.3 ± 0.67	4.93 ± 0.31
candesartan cilexetil	26.4 ± 1.46	15.6 ± 0.54
carbamazepine	34.5 ± 1.06	nd
cinnarizine	22.7 ± 1.83	nd
clofazimine	15.9 ± 0.83	nd
clotrimazole	44.1 ± 3.01	33.2 ± 3.70
danazol	29.8 ± 0.50	24.4 ± 1.91
diflunisal	157.9 ± 6.54	139.3 ± 7.14
dipyridamole	9.57 ± 0.29	nd
disulfiram	88.8 ± 3.66	85.5 ± 3.27
ethinylestradiol	163.9 ± 10.1	144.4 ± 14.4
felodipine	125.1 ± 6.23	104.6 ± 8.22
fenbendazole	2.07 ± 0.09	1.75 ± 0.06
fenofibrate	101.3 ± 5.76	116.2 ± 4.43
fenofibric acid	58.4 ± 2.59	39.5 ± 0.42
glibenclamide	11.2 ± 1.01	2.82 ± 0.58
griseofulvin	9.70 ± 0.36	nd
halofantrine	27.9 ± 0.79	38.3 ± 1.60
haloperidol	11.3 ± 0.82	17.3 ± 0.82
indomethacin	71.6 ± 4.57	80.6 ± 3.69
itraconazole	1.92 ± 0.29	2.50 ± 0.41
mefenamic acid	30.7 ± 0.89	nd
naproxen	119.9 ± 2.97	nd
niclosamide	44.1 ± 1.75	47.9 ± 1.24
noscapine	12.3 ± 0.25	12.8 ± 0.40
perphenazine	71.7 ± 3.04	69.8 ± 1.92
praziquantel	45.4 ± 3.51	nd
progesterone	41.1 ± 1.27	35.0 ± 1.23
saquinavir	≥ 45.9	nd
sulfasalazine	13.1 ± 1.02	6.35 ± 0.33
tolfenamic acid	70.6 ± 3.87	50.3 ± 1.42
toltrazuril	19.7 ± 3.11	10.7 ± 1.07
min	1.92	1.58
max	163.9	144.4

^aThe Cremophor EL data is shown here, as well as in the article, for direct comparison with Cremophor ELP.

Table S13. Explanation of calculated DragonX 6.0.16 (Talete, Italy) descriptors applied in the final PLS models

Descriptor	Description	Block
B04[N-O]	Presence/absence of N - O at topological distance 4	2D Atom Pair
B07[N-O]	Presence/absence of N - O at topological distance 7	2D Atom Pair
B10[C-O]	Presence/absence of C - O at topological distance 10	2D Atom Pair
CMC-80	Ghose-Viswanadhan-Wendoloski CMC drug-like index at 80%	Drug-like index
G2s	2nd component symmetry directional WHIM index / weighted by I-state	WHIM descriptor
GATS1p	Geary autocorrelation of lag 1 weighted by polarizability	2D autocorrelation
GATS8s	Geary autocorrelation of lag 8 weighted by I-state	2D autocorrelation
HATS6i	Leverage-weighted autocorrelation of lag 6 / weighted by ionization potential	GETAWAY descriptor
HATS7e	Leverage-weighted autocorrelation of lag 7 / weighted by Sanderson electronegativity	GETAWAY descriptor
JGI6	Mean topological charge index of order 6	2D autocorrelation
MATS7e	Moran autocorrelation of lag 7 weighted by Sanderson electronegativity	2D autocorrelation
Mor18i	Signal 18 / weighted by ionization potential	3D-MoRSE descriptor
Mor26i	Signal 26 / weighted by ionization potential	3D-MoRSE descriptor
R6e+	R maximal autocorrelation of lag 6 / weighted by Sanderson electronegativity	GETAWAY descriptor
SAacc	Surface area of acceptor atoms from P_VSA-like descriptors	Molecular property
TDB06s	3D Topological distance based descriptors - lag 6 weighted by I-state	3D autocorrelation

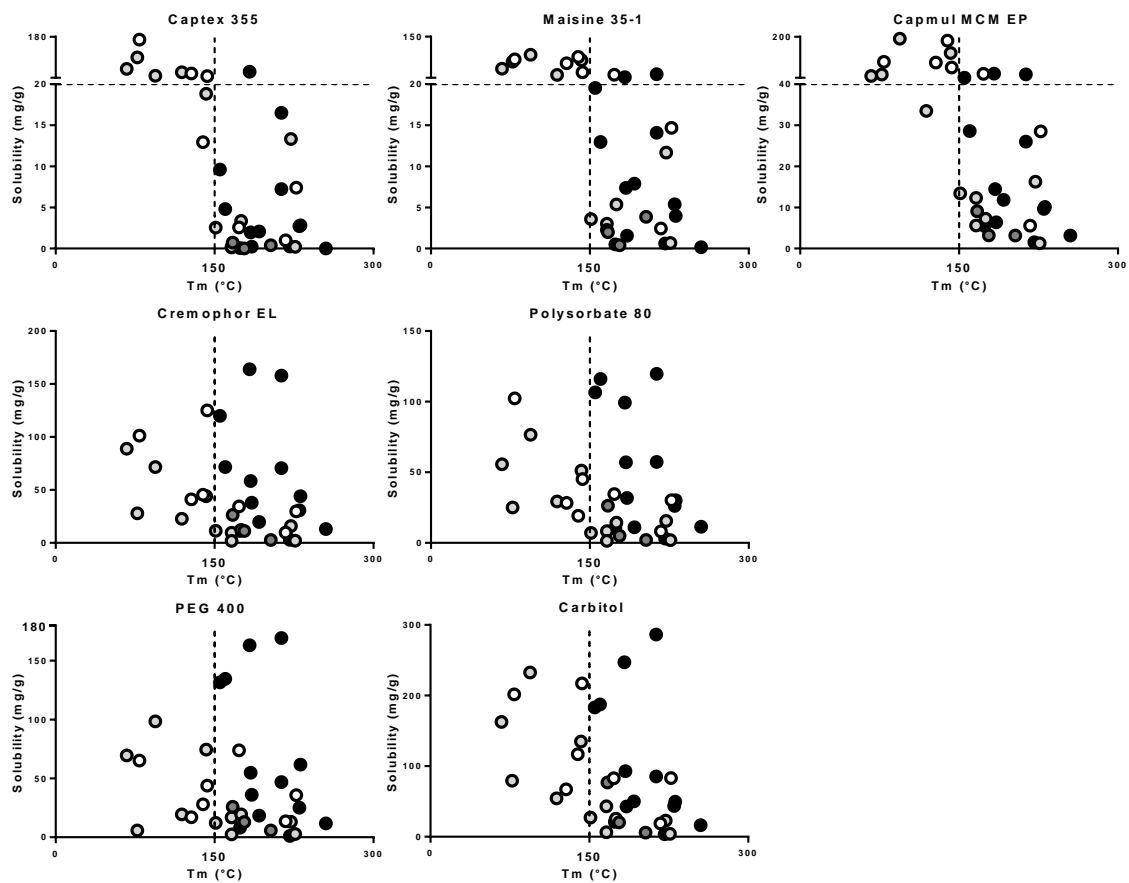


Figure S11. Relationships between solubility of drug compounds in key excipients of lipid-based formulations and melting point. Black circle (acid), dark gray circle (ampholyte), light gray circle (base) and white circle (neutral).